The Characterisation and Modelling of Polymer Bonded Energetic Systems

William G. Proud
Institute of Shock Physics, Royal Schools of Mines,
Imperial College London, London, SW7 2AZ, UK

e-mail: wproud@imperial.ac.uk

ABSTRACT

Polymer-based systems are widely used in energetic systems, in warheads, motors, explosive trains and pyrotechnics. They are suited for applications where factors such as weight, strength and formability need to be balanced. In general they have non-linear mechanical properties which are highly-temperature dependent and strain-rate sensitive. In this paper a number of low to high-rate characterisation techniques are presented. Results polymer bonded explosives (PBX), propellants and polymer bonded sugars (PBS) are reviewed.

The importance of predictive modelling, using a limited empirically measurable parameters is of increasing importance. Advances, especially those models which start from molecular considerations, provide methods for prediction of polymer and polymer composite behaviour which allows a more focussed series of validation experiments to be conducted. This approach will be illustrated by comparison of results with predicted constitutive equations.

1.0 INTRODUCTION

The behaviour of polymer-bonded energetics materials over a range of stress and strain-rate regimes is linked to more fundamental understanding of polymer behaviour. Polymers are widely known to non-linear and highly temperature dependent compared to *e.g.* metals.

The field of high strain-rate experimentation and modelling has expanded greatly in recent years, with the increase in high-speed diagnostics allowing sub-microsecond and in some cases femto-second time resolution to become commonplace. Increased use of predictive modelling with the implied increase in the number of materials and materials models has provided a significant drive for well-controlled experiments and physically-based models. This forms a development circle involving experiment, theory and numerical methods. The use of multiple diagnostic systems on a single experiment, e.g. stress gauges, high-speed photography and flash X-ray systems, has provided much improved understanding of the qualitative and quantitative processes occurring at short time scales and has made a large contribution to more physically based models.

Table 1 lists some of the more widely used techniques in the strain rate characterization of materials. A review on these techniques applied to a wide range of materials has been published by the author, in collaboration with colleagues, elsewhere [1]. The main effect of increasing the strain rate is that the transient stress levels increase and the sudden delivery of energy allows processes with high activation energies to be accessed. In many of these techniques those processes, which operate on long time scales, e.g. thermal diffusion, which are significant under quasi-static loading and in some hazard scenarios, do not have time to occur.

It is generally found that yield and fracture stresses increase with increasing strain rate [2]. The increase in failure stress is very marked at strain rates above 10^3 s^{-1} and the effect of inertia becomes significant. Ultimately the response changes from one where the sample can be assumed to be in stress equilibrium to one of a wave with associated 1-D strain moves so quickly that the material does not have time to move laterally, as seen in shock waves.

Strain rate	Equipment	*Stimulus duration*	*Comment*
$10^{-6} – 10^{-2}$	Instron	100s of seconds	Quasi-static loading
$10^{+2} – 10^{+3}$	Drop weight	10s milliseconds	Generally used to determine impact ignition thresholds
$10^{+2} – 10^{+3}$	Hopkinson bars	100s microseconds	Compression, tension and torsion loading. Extensively used for PBX formulations. Constitutive models.
$10^{+4} – 10^{+5}$	Miniature Hopkinson bar	10s microseconds	For fine grain materials or single crystals. Generally metals
$10^{+3} – 10^{+6}$	Taylor impact	10s microseconds	Sometimes used for metal jacketed energetic samples
$10^{+5} – 10^{+8}$	Plate impact	microseconds	Pressures and durations similar to that of gap tests. Laser driven flier plates have sub-microsecond duration high-intensity shocks

Table 1: High Strain Rate Regimes and the Associated Equipment.

In addition, standard thermal and mechanical techniques, such as differential thermo-mechanical analysis (DMTA) are widely used in the polymer community and provide insight into the molecular-level processes occurring in polymer-based systems.

A brief survey of the literature will reveal a number of models available, all with greater or lesser degree of empirical parameters. Historic spring-dashpot models are used with some degree of success in some areas, there are numerous semi-empirical models, however, there is a great drive to use models which are based on the fundamental structure of the polymer as in the group interaction model [3] is proving a fruitful area

Polymer bonded granular composites, such as PBX, propellants and PBS formulations have further complexity in the presence of interfaces between binder and filler material. This can have the effect of increasing composite strength compared to that of the polymer, while a potential problem is that de-bonding between the filler and the binder can produce extra failure points in the system.

The following sections of this paper illustrate some of the material characterisation seen across a wide range of strain-rates, ultimately linking to the Porter-Gould model of polymer behaviour. This model is chosen in particular as it has been applied to a range of polymer-bonded energetic systems with success and, in addition, because it is populated using parameters which can be independently determined from hazard and IM tests.

2.0 THE STRUCTURE OF POLYMER BONDED SYSTEMS – THE BINDER

In addressing the modelling of polymer-bonded materials it is important to know what the structure of the material is [4]. It may be found that the production method can produce fine-grains of material which intimately mix with the binder, thus providing a modified, strengthened and potentially more brittle binder. Evidence for this emerges from compression and tension studies on polymer-bonded systems but can also be clearly seen using microscopy techniques.

Atomic force microscopy (AFM) is one of the family of probe in its basic form, the technique consists of the sample being scanned by a miniature cantilever with a sharp tip (figure1). The in surface mode the tip apex is in continuous contact with the surface and the cantilever flexes as it is moved over the sample. The degree of flexure is monitored and so surface topography is recorded. Materials such as silicon carbide, diamond and metals have been used as the tip. The high resolution of AFM relies on the tip having a curve radius of the order of 25 nm, this has allowed atoms in a metallic matrix to be observed and the double helix of DNA to be directly detected.

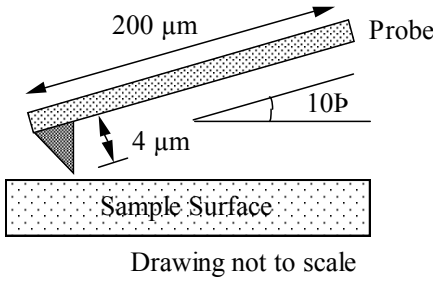

Figure 1. The arrangement of AFM probe and sample surface

For soft materials such as polymers and biological samples, the high contact forces cause the sample to be deformed this can lead to sample damage as well as inaccurate images. This lead to the development of the tapping mode of image acquisition [5]. In this mode short intermittent contact is made between the tip and the surface by oscillating the cantilever. One additional effect of doing this oscillation is that the resonant frequency of the cantilever changes with the surface force acting on it. This produces a change in the phase of the cantilever and the oscillator driving the tip. In general, the magnitude of the force between sample and tip decays with tip-sample distance differently for chemically distinct materials; this allows compositional variation to be detected. Maganov and Reneker reviewed such AFM studies of polymers [6]. The mechanical properties of polymers have been probed using the AFM tip as an indentation probe [7 8] and the damage produced by mechanical action has received attention7. Some studies have been performed with AFM on energetic systems either looking at the fracture surfaces of TNT [10], nanostructures of RDX [11] or at impact-induced ignition sites in RDX [12].

The material studied here consisted of a polyeurathane bound system in which the loading of HMX exceeded 90 wt% is studied thus representing a generic solid polymer system. Figure 2 shows the topographic structure for a field of view of 50 µm x 50 µm. An explosive crystal occupies the top left-hand corner of the image, while another crystal occupies the lower left-hand edge. In the region between these two crystals, a region of smaller explosive crystals and binder is seen. The explosive crystals vary greatly in size and shape.

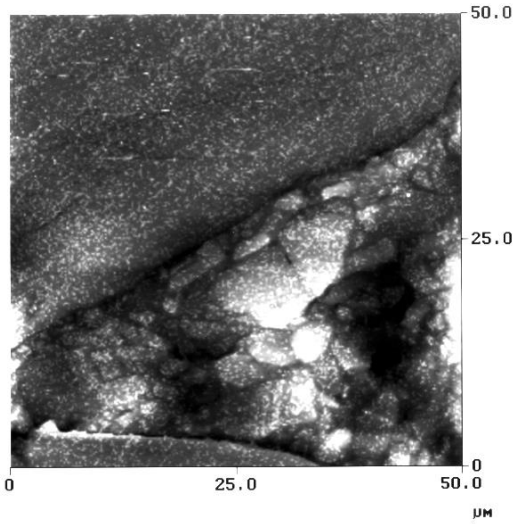

Figure 2 Topographic image of a 50 µm x 50 µm area of polyureathane HMX system. The surface is flat to 350 nm. Part of an explosive crystal is at the top left-hand side, the edge of another crystal forms the lower edge of the image. The region between these crystals is the binder rich area. Taken from [4]

A closer inspection of the binder-rich region of the PBX is shown in figure 3. There are three features to be noted in this image: (a) the pebble like structures on the surface, 50 to 100 nm long, some of which appear to be fractured; (b) the flat region between the pebbles, and (c) the darker regions seen predominantly in the phase image.

There are several possible explanations for these structures, however, the most likely is that the pebbles are small, hard explosive crystals, the flat region is the bulk of the binder and the dark regions in the binder are regions of soft binder, possibly a less cured area. It should be noted that these dark regions are seen in the phase image but are hardly noticeable in the topographic image and are an indication of a different chemical or mechanical nature. The fine-grained material is not the polishing medium, as this has been examined and found to be angular and is very much tougher than the relatively soft PBX surface.

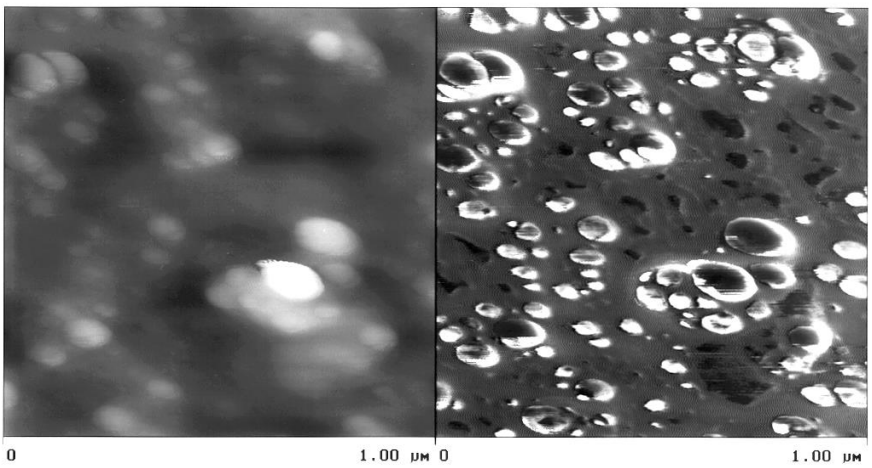

Figure 3. A binder-rich area. Field of view 1 µm x 1 µm. Topographic image on the left, phase image on the right. The phase image indicates hard pebble like inclusions along with softer regions in the binder matrix. Taken from [4]

3.0 THE STRUCTURE OF POLYMER BONDED SYSTEMS –THE ENERGETIC FILLER

As well as the binder material the energetic filler has a large influence on the properties of the material, mechanically and in terms of reaction. Materials such as iRDX were produced in the mid-1990s and have produced considerable interest in because of the desire for insensitive munitions. In recent years many studies have been carried out to look for links between sensitivity and morphology. Variations in shock sensitivity between different batches as great as 50% have been measured. As well as materials purity, many aspects of the morphology have been suggested as crucial factors in hotspot generation, including surface roughness and voids, internal defect population, and dislocation motion [13-15] .

Research by Czerski et al. [16] the void content of crystals in different batches of energetic powders and compacts was considered in relation to shock sensitivity. For the smallest size class, the most sensitive crystals had only 1 or 2 voids per crystal, although a few crystals with many voids (up to 20) skewed the average (figure 4). For both size classes studied, it was observed that the most sensitive crystals contained the fewest internal voids. This suggests that either the void content is not the dominant mechanism or, less likely, that internal voids may act to suppress shock to- detonation transition. In view of the large volume of literature correlating void content with sensitivity, it seems that for RDX and HMX, in the small scale gap test used, factors other than void content dominate. There are some confirmatory results of the greater importance of surface defect density on the crystal over internal crystal voids in PBX systems [13,14].

Figure 4: Images of energetic crystals from different batches, studied using optical microscopy with crystals submerged in index-matched fluid, to show internal structure more clearly. Less voids required higher shock pressures to cause reaction [16].

The increased use of computed tomography on polymer-bonded energetic systems is increasingly used. It provides a method of determining the particle size distribution, internal flaws and voids, both in the binder, the crystals and the interface between the two. The main limitation is the size of the volume element (voxel) that can be determined. This type of data is essential in populating micro-mechanical models [17-19]

4.0 DROP-WEIGHT

Conceptually a drop weight is a very simple device, gravity is used to accelerate a mass onto a sample and the resulting deformation and damage pattern observed. As with many experimental techniques care has to be taken with a number of experimental parameters; the geometry of the mass and sample, the contribution of friction at the interfaces, the relative movement of the upper face of the sample compared with lower face of the sample. Gauge traces from drop-weight systems are also notorious for the amount of “ringing” or oscillations seen on the signal, the result of a combination of mechanical and electrical resonance in the system. However, accurately aligned drop-weight experiments give extremely useful quantitative data e.g. stress-strain curves. Drop weight studies on polymer systems are illustrative of a number of phenomena that can be seen. Stress localisation and shear bands may also form due to the geometry of the sample. Heat sensitivity films have also been used to track the rapid, transient heated associated with the drop-weight impact [20]. Illustrative examples can be seen in figure 5 taken from [21].

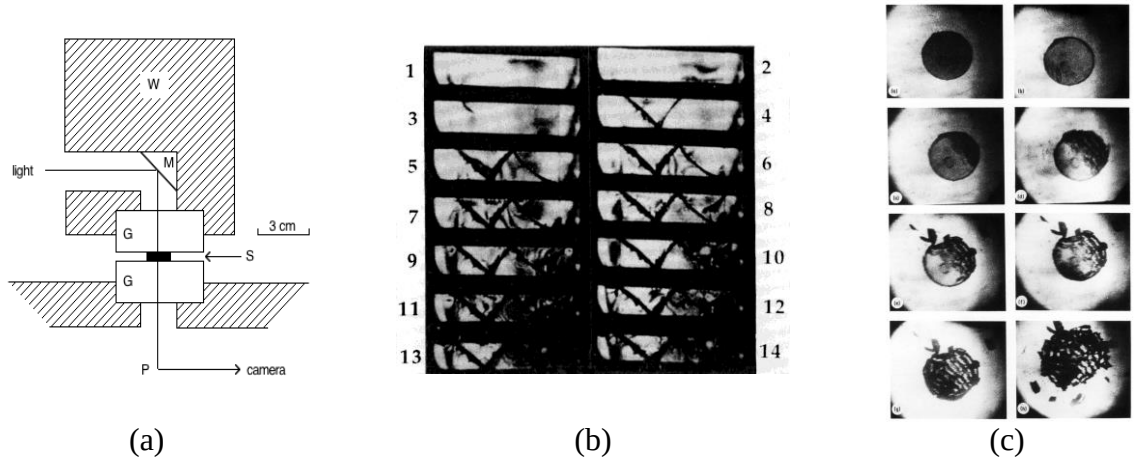

(a) (b) (c)

Figure 5 (a) Schematic of the high-speed photography drop weight.W weight, M mirror, G glass anvil, S specimen, P prism. Mass of drop weight = 5.545 kg. (b) Selected frames, 20 microsecond interframe time shows the shearing and fracture in a polystyrene sample (22.5 x 7.3 x 3 mm side lengths) during drop weight impact. (c) Along impact view. Impact on a 5 mm diameter, 1 mm high disc of PS. Times after frame (a): (b), 35 μsec; (c) 42 μsec; (d) 49 μsec; (e) 189 μsec; (f) 196μsec; (g) 203 μsec; (h) 259 μsec.

5.0 HOPKINSON BAR

In order to transmit stress pulses into samples rods can be used as wave guides [1]. The rod can transmit a stress into a sample, the specimen being taken to large strains. The basic idea of the split Hopkinson pressure bar (SHPB) is that the specimen is deformed between two bars excited above their resonant frequency and chosen so that they remain elastic (small strains). This means that strain gauges can be used repeatedly to measure the signals in the bars (strain gauges normally have small failure strains). Dynamic loading is produced either by striking one end of one of the bars (the input bar) or by statically loading a section of the input bar held at some point by a clamp and then releasing the clamp so that the load propagates to the specimen. Compression bars are nearly all of the dynamically loaded type and represent the most common and conceptually easiest system – a schematic is shown in figure 6.

In many respects the strain rate regime from 10^2 – 10^4 s^{-1} represents a challenge in understanding. While most materials show an increased yield strength with strain rate there is evidence of a fall in yield strength in a number of polymers in this region, followed by a rise at the higher rates as seen in figure 7.

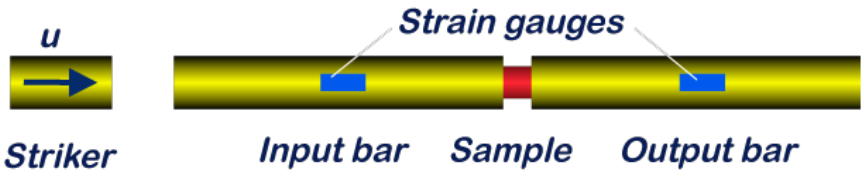

Figure 6. Schematic of a compression SHPB system

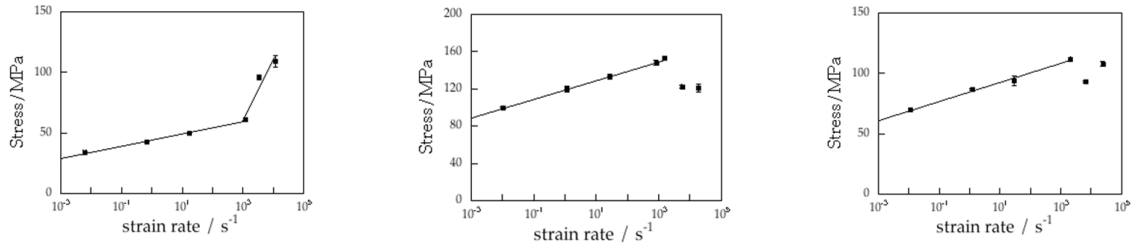

Figure 7. Yield stress versus strain rate for a number of polymers (a) A "normal" response seen in acrylo-nitrile-butadiene (ABS) such a response trend is seen in metals and geological materials (b) PEEK, and (c) Polycarbonate, showing a marked and reproducible drop at in yield stress at the higher rates, taken from [22]

The effect of the molecular relaxation processes in this regime has been addressed for polycarbonate and polyvinylidene diflouride [23]. In this study the use of stress rate temperature mapping is emphasised a suitable method for understanding these polymer systems.

In granular systems composite systems this is further complicated by processes such as debonding, fracture nucleating in the binder and cracking of the filler material. Macro-properties sometime show trends in remarkable agreement with those seen in metallic systems. In the mid 2000's the effect of grain size on the high rate mechanical properties of an ammonium perchlorate (AP)/hydroxyl-terminated polybutadiene (HTPB) PBX was studied. This PBX consisted of 66% AP and 33% HTPB by mass. The AP was available in four different crystal sizes: 3, 8, 30 and 200–300 mm. The effect of grain size was most clearly seen at low temperatures (figure 8) the effect of particle size on the flow stress of the material is linear in $1/d^{1/2}$; where d is the particle size (figure 9). This has been subject to further investigation to determine if the particle size or the particle separation is dominant, this research is on-going e.g. [24].

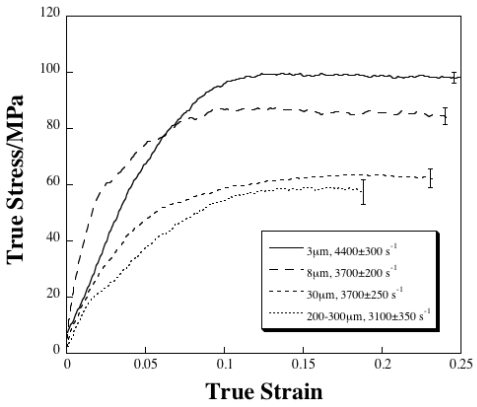

Figure 8 Effect of particle size on yield stress at -60°C

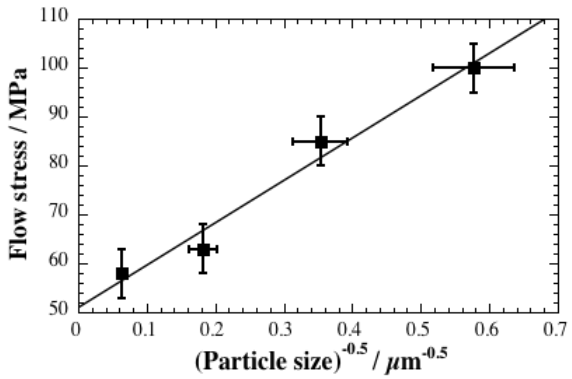

Figure 9 Plot of the flow stress versus the reciprocal of the square root of particle size for the data of figure 8. Digital Speckle Photography

With the increased use of high-speed imaging other research has concentrated on tracking the deformation of the sample during the loading process [25] the technique of optical cross-correlation has been used. This is a method that, in broad terms, compares the movement of random pattern, either naturally present, as in the case of large grain-size PBXs, or painted onto the surface. Typical output of this technique can be seen in figure 10. This analysis technique has also been applied to granular polymer composites over a range of strain rates [26, 27].

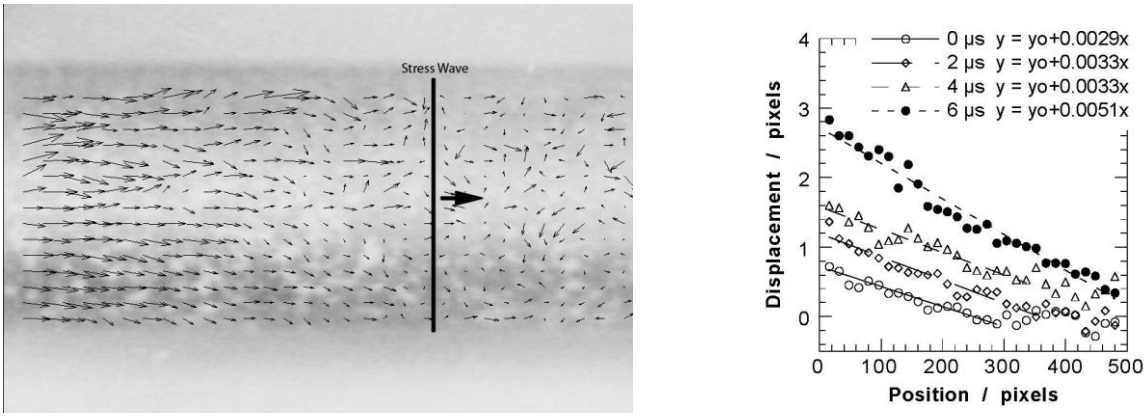

(a) *(b)*

Figure 10. (a) Displacement quiver plot for a stress wave passing through a cylindrical specimen of polycarbonate in a compression Hopkinson Bar System. The stress pulse causes compression in the sample. The exposure time of this image was 1 microsecond, thus freezing the motion. Image cross correlation was used to see the wave front. (b) Plot of displacement against position along a polycarbonate specimen, at four different times during loading. The horizontal scale is 53 pixels mm^{-1}, so the movement of the wave front agrees with a wave speed of 1.4 mm μs^{-1}.

Samples of an inert PBX simulant, a polymer-bonded sugar (PBS 9501), were sprayed with a dilute solution of silver dag, to give a fine, silver speckle pattern. High-speed photographs were taken, during a compression test, using an Ultra-8 camera, and analyzed as described in [27]. The evolution of displacement on the surface of a typical specimen, relative to the undeformed frame, is given in figure 11. The arrow on the frame at 24 μs shows the onset of strain localization, before surface cracks are visible in the next frame. Comparison to the stress-strain curve in figure 12 shows that the first sign of localization corresponds to the peak stress. This means that that localization, or cracking, precedes strain softening in this material.

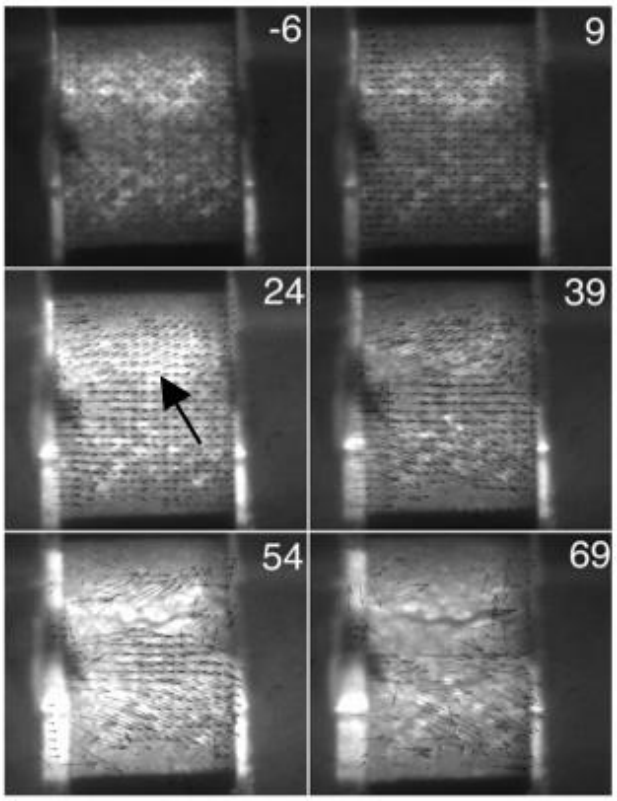

Figure 11. Displacement Evolution at 1420 s^{-1}. Exposure time 2 µs, frame times shown relative to arrival of stress wave. The arrow in frame 24 indicates the onset strain localisation.

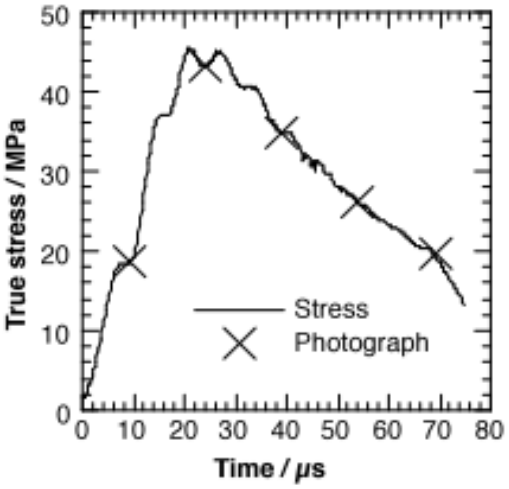

Figure 12. Stress-time plot for the specimen of PBS 9501 in Fig. 11. The frames shown in figure 11 are indicated by crosses in the stress-time curve.

The speckle data were, where possible, also used to calculate global surface strain fields in the specimens in longitudinal and radial directions and thus an apparent Poisson's ratio at different strains was calculated. Overall these measurements show, during deformation, an early onset of specimen fractures producing voids in the sample: Mechanically the area of the *specimen* is not the same as the load bearing area of material [28]. Therefore, the true stress in the material may be better represented by assuming volume conservation in the material not volume conservation of the specimen. However, to measure volume conservation in this way would require significant technique development in dynamic tomography for example. In a practical sense, it is encouraging that the key features of the mechanical behaviour occur at small strains, where the difference between the stress-strain curve calculated assuming volume conservation and the true volume of the sample, will be small.

On-going research using samples subject interrupted loading and followed by computed tomography is likely to provide improved insight into the underlying damage mechanisms. This type of data provides a stringent test for constitutive models [29].

6.0 PLATE IMPACT

At the very high strain-rates, shock studies are used. A shock wave is a travelling wave front, which has a discontinuous adiabatic jump in state variables. The loading time is short compared to the inertial response, pressure pulses propagate through the body to communicate the presence of loads to interior points, and thus, the material inertia is important. A detailed review on shock wave physics was published by Davison and Graham [30]. The most common experimental method of inducing a shock wave in a target is by plate impact as illustrated in figure 13. The stress components can be measured by commercially available piezoresistive manganin gauges, which have been calibrated [31,32] for 1-D shock loading. The particle velocity can either be measured using wire gauges, which operate by applying a constant magnetic field normal to the gauge [33], or by a velocity interferometric system, such as VISAR [34] or phase Doppler velocimetry [35].

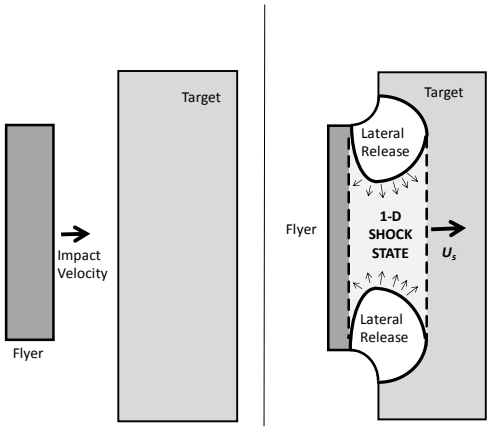

Figure 13. The plate impact experiment. A flier plate strikes a target causing a shock wave to move at a velocity (U_s) through the target and the impactor. The region of high pressure 1-D shock reduced by lateral releases as well as along-axis longitudinal wave reflections

In many solids, under shock loading there is an initial elastic region, up to the so-called Hugoniot elastic limit (HEL). Even in relatively simple cases, such as metals, below the HEL, strain and strain rate hardening as a result of dislocation accumulation is often seen. In heterogeneous materials and most polymers, a clear elastic limit is harder to determine due to the ramping caused by the differing impedances of the components or the material structure. In addition, as the passage of the wave is adiabatic, the temperature can increase dramatically. As a result, polymers may exhibit thermal softening effects as a result of this heating along with a counteracting hardening effect caused by the increased strain rate and the limited time for molecular motion to accommodate the stimulus.

At very high stress, ~20GPa, the energy deposited is sufficient to cause many polymers to chemically decompose. For some polymers a “kink” can be seen in the shock velocity – particle velocity Hugoniot. This kink occurs between 10-14 GPa in density polycarbonates for example (figure 14). A mechanism based on the removal of free volume between polymer chains has been proposed but no predictions have been made based on this hypothesis. Such a kink is not seen in high density polyethylene.

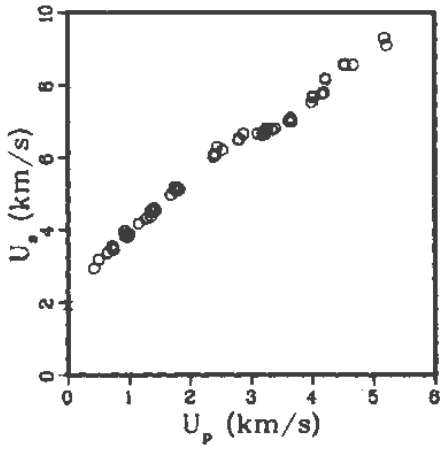

Figure 14. The shock velocity-particle velocity response of a polycarbonate. The plateau seen in the region of U_s = 6.8 km s^{-1} has been associated with the removal of free-space between the polymer chains. Taken from [36]

A similar kink is seen in poly(styrene). Porter and Gould [37] proposed that this kink is due to an activated change in structure whereby the aromatic ring transforms into a triangular prism. Molecular mechanics can predict the equation of state of polymers from their structure alone [23] and this technique has been used to predict pressure-volume for the two structures: aromatic ring and triangular prism. The prediction is compared with experimental data in Figure 15. Molecular mechanics also allows prediction of the activation energy of such a structural change, via an energy density, and this equates to a pressure of around 20 GPa, the 'kink' seen in [36].

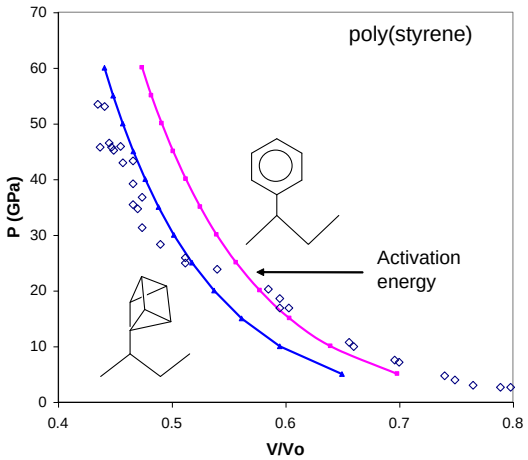

Figure 15: Comparison between predicted pressure-volume behaviour of two structures in poly(styrene) and measured data

Significant effort has been made to understand the material response both in terms of the strain-time records seen and also in the recovery of shocked samples for post impact analysis [39]. Here both strain-rate hardening and softening was seen in PTFE samples, depending on the conditions used, re-shocking of the sample material had a significant effect and there was a marked difference in the crystallinity of the recovered material.

7.0 INTERNAL MOTION IN SHOCK PROCESSES - DIGITAL SPECKLE RADIOGRAPHY

Digital Speckle Radiography (DSR) is equivalent to Digital Speckle Photography (DSP), described earlier. However, DSR makes use of X-rays and the placing of a lightly populated, <30%, layer of X-ray opaque particles within samples. This allows for the measurement of internal deformation in optically opaque materials. Here, a PBS, based on granulated sugar in a hydroxy-terminated polybutadiene (HTPB) matrix, was used. The speckle field was by a layer of lead particles, 500 μm, on the central axis of the fill, covering 20 % of the area. A Scandiflash 150 keV unit produced a flash of x-rays in a 70 ns pulse. The X-rays, after passing thought the target, impinged upon medical grade intensifier screens and film, which was subsequently digitally scanned. In additionally to single shock loading, an experiment was performed in which the sample was doubly shocked, using a composite flier of a polycarbonate plate backed by a copper plate. Double shock scenarios have important implications for explosive initiation. Figure 16 shows the X-ray image which capturing the shock-loading process. The projectile has just begun to penetrate the target. Also visible in the image is a fiducial speckle field, used to align the scanned images. Also visible is the silhouette of a British 1 penny piece, which acts as a scale bar (diameter 20.32 mm).

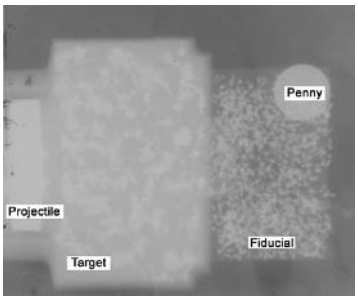

Figure 16: Flash X-ray of impact experiment Projectile traveling left to right. Taken from [44]

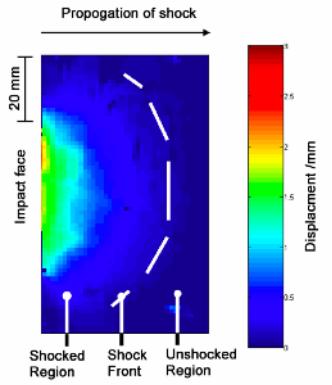

Figure 17: u-component data from plate impact experiment.

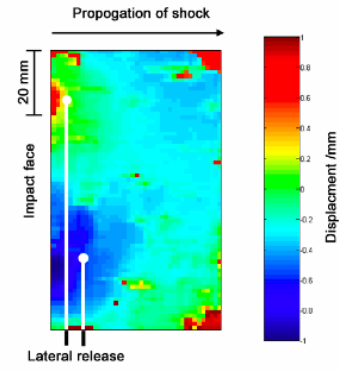

Figure 18: v-component data from plate impact experiment.

In the analysis, the u-axis is parallel to the projectile axis, and the v-axis is perpendicular. Figure 17 shows the u-component of displacement, the shock wave is clearly visible. The curved nature of the shock front is due to the lateral release of material from a shocked to an unshocked state. The lateral release waves originate from the radial edges of the plate projectile where the material is no longer loaded uniaxially, and will eventually negate the propagating shock wave. The lateral release, producing lateral 'v' displacement is shown in figure 18.

From the displacement curves and knowledge of X-ray trigger times, the shock velocity was estimated as 1.6 km s^{-1} for an impact at 300 m s^{-1} and 2.4 km s^{-1} for an impact at 600 m s^{-1}. This is entirely expected in shock studies where wave speed increases with increasing stress levels. In addition the data was used to determine the strain produced by the shock waves: 4.0 ± 0.1 % for the impact at 300 m s^{-1} and 7.3 ± 0.1 % for the impact at 600 m s^{-1}.

With the composite impactor a double, or stepped, shock wave was sent through the target. The resulting displacement map is shown in figure 19. Region I is unshocked material. Region II is material subject to the first shock from the polycarbonate is strained by 5.5 ± 0.1 %. Region III is material subject to double shock loading, first by polycarbonate and then copper strains to 60 ± 5 %. This data has been used both to populate and validate material models [40].

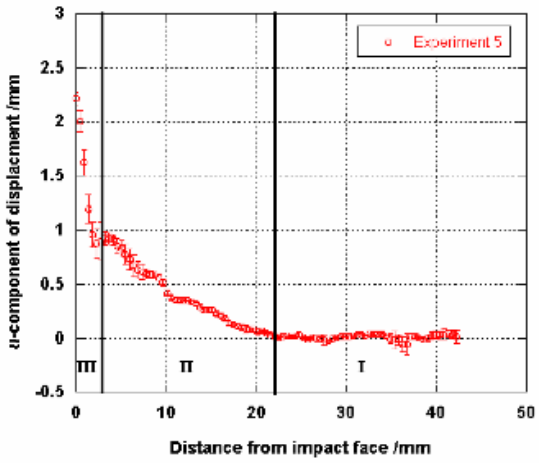

Figure 19. Displacement measured in PBS material subject to a stepped shock wave.

8.0 TEMPERATURE TIME SUPERPOSITION

The previous sections have highlighted some of the techniques used and have illustrated some of the difficulties involved. Without adequate knowledge of the underlying system processes it would be difficult to encapsulate the behaviours into a coherent model. However, much effort has been made into consideration of the variation of temperature and the time and strain rate response of the material. This allows the polymer behaviour to be explained in a coherent fashion thus leaving the processes of fracture and damage more visible in the data.

This can be illustrated by considering the temperature time response of a polymer bonded energetic system. This study is one of the few that represents a complete study across a wide range of strain rates and temperatures [41,42].

In this study the compressive strength of the energetic composition EDC37 was measured at a temperature of 293 ± 2K over a range of strain rates from 10^{-8} to 10^{3} s^{-1}, and at a strain rate of 10^{-3} s^{-1} over a range of temperatures from 208 to 333 K. The results show that failure stress is a monotonic function of applied strain rate or temperature, which is dominated by the relaxation properties of the polymeric binder; this is confirmed by dynamic mechanical thermal analysis performed on both EDC37 and its binder. Similarities between the compressive strain rate/temperature data sets can be understood by temperature–time superposition; data collected at a strain rate of 10^{-3} s^{-1} over a temperature range 208 to 333K were mapped onto a plot of strain rate dependent strength at 293 K, using an empirically determined sensitivity of −13.1 ± 0.3K per decade of strain rate. Sample size had a modest effect on the stress–strain behaviour; small length to diameter ratios gave results consistent with an increased degree of confinement. Samples taken to large strains exhibited strain localization in the form of shear bands. Figure 20 shows the main experimental results used in this study: the similarity in trends is obvious.

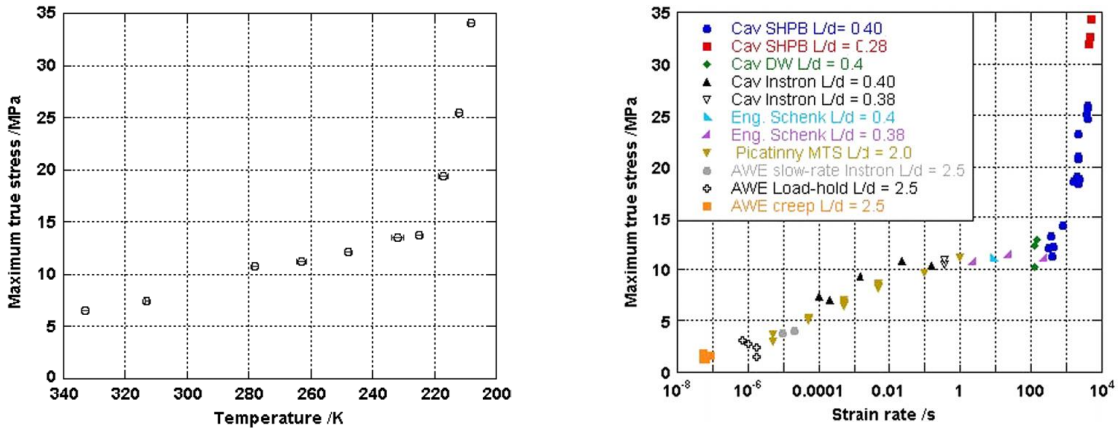

(a) (b)

Figure 20. Yield strength of a granular composite at (a) a fixed 10^{-3} s^{-1} strain rate, varying temperature (b) failure stress as a function of strain rate tested at 293 K.

9.0 CONSTITUTIVE MODELLING

The prediction of constitutive models for polymer composites is facilitated by the plethora of good composite models available in the literature. These rely, however, on knowledge of the properties of the components and an understanding of how the presence of stiffening phases in a polymer matrix changes those properties. Conventional constitutive models for polymers cannot be used reliably for that purpose particularly at high rate and for high volume fractions of filler.

Group Interaction Modelling [3, 43] has shown that the properties of polymers at low rate, high rate and under shock can be reliably predicted from the chemistry of the polymer alone. This also allows phase interactions to be included so as to fully inform composite models. The basis of the approach is to determine the energy-volume response of the interacting groups and to understand the degrees of freedom involved in those interactions. This allows the loss spectrum for the polymer to be determined together with its changes with temperature and rate.

A volumetric potential well is constructed for the interacting system and this predicts bulk modulus, density, thermal expansion coefficient and glass transition. The heat capacity as a function of temperature is predicted from the one dimensional Debye temperature and the degrees of freedom. Relaxation phenomena alter the transition temperatures with rate and a Vogel-Fulcher form is used to determine this dependency. The main advantage of this approach is that no fitting is required. Figure 21 shows the prediction of modulus and loss spectrum for poly(carbonate).

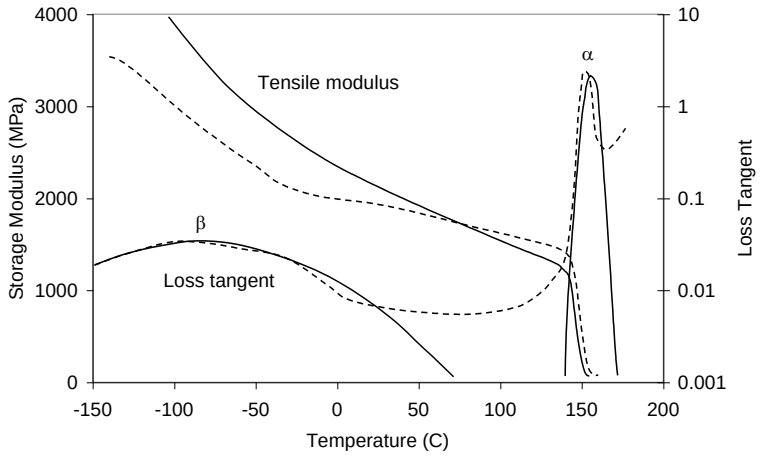

Figure 21: comparison between predicted and measured loss tangent and tensile modulus at 1Hz for poly(carbonate)

Once the loss spectrum is known then it can be combined with the predicted modulus to predict the stress/strain response in tension. Poisson's ratio gives the response in compression. This allows certain important experimental outputs such as yield stress to be predicted. Figure 21(a) shows the prediction of yield stress vs. rate at room temperature for two common polymers: poly(carbonate) and poly(methylmethacrylate) and compares it with available data. Figure 22(b) shows the comparison with model and experiment for a polymer-bonded energetic system.

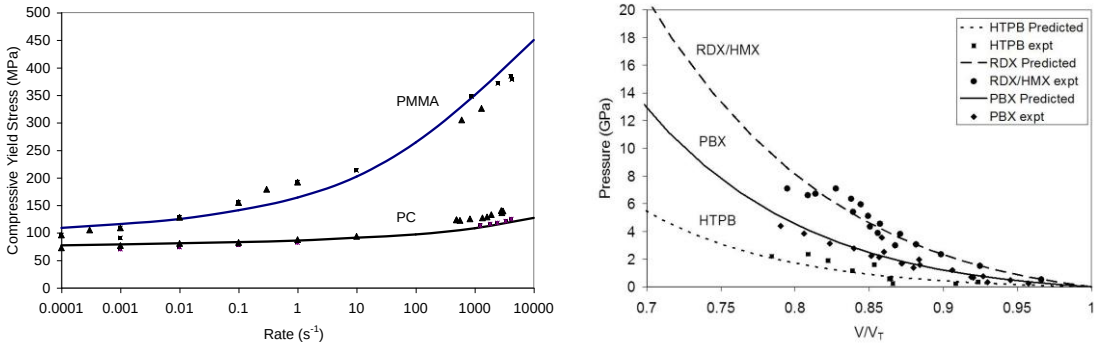

(a) **(b)**

Figure 22: (a) Prediction of variation of compressive yield stress with rate for two common polymers across strain rate (b) Pressure volume curves predicted for a polymer-bonded energetic material.

10.0 CONCLUSIONS

In this review the response of energetic-polymer composites has been shown to be complex. A number of failure processes can occur on short timescales. The mechanical properties are strongly dependent on the binder behaviour which in term links to temperature and the underlying molecular processes.

In a variety of polymer and polymer composites the application of temperature-time (frequency) shifts is shown to explain some of the behaviours seen. Much of the stress-strain curve can be explained through these phenomena. In a way this is unsurprising, the polymer is the softer component in most of these systems and so accommodates the majority stress and so heats more than the filler particles.

The main challenge in this area remains in quantitatively measuring the damage level induced by such loadings, accommodate it into a coherent model and link it to a reaction model.

11.0 ACKNOWLEDGEMENTS

The author acknowledges the large number of colleagues, students and collaborators, who have supported and developed the techniques in this review, mainly at the Cavendish Laboratory, University of Cambridge. Principal inspiration and guidance was provided by Prof. J.E. Field. Other colleagues included Drs. S.M. Walley, P.J. Rae, J.E. Blazer, S.G. Grantham, C.R. Siviour, H.T. Goldrein, D.J. Chapman, H. Czerski, D. Drodge and, in particular D.M. Williamson. Mr. SJP Palmer provided innovative and determined technical support to many of these projects. Indispensable technical assistance was provided by D. Johnson, R. Marrah, R. Flaxman, K. Fagan and others. EPSRC, QinetiQ, [dstl], Orica, AWE and MoD, provided the support for much of this research. Drs and Profs. I.G. Cullis, A.S. Cumming, P. Gould, P.D. Church, D. Mullenger, P. Haskins, M. Cook, M. Braithwaite, all provided programmatic guidance. This list is not exhaustive and the author apologises for any omissions. The Institute of Shock Physics acknowledges the support of the Atomic Weapons Establishment, Aldermaston, UK an Imperial College London. Readers are asked to consult the original papers to find greater detail and attribution.

12.0 REFERENCES

[1] Field JE, Walley SM, Proud, WG, Goldrein, HT, and Siviour, CR,. IJIE, 30 (2004),, 725-775.

[2] Meyers, MA, Dynamic Behavior of Materials. New York, Wiley Interscience. 1994

[3] Porter D., Gould P.J, IJSS 46 (2009) 1981–1993

[4] Proud W.G., Palmer S.J.P., Field J.E., Kennedy G. and Lewis A., AFM of PBX Systems, Thermochimica Acta, Vol. 384 (2002) 245-251

[5] P. K. Hansma, J. P. Cleveland, M. Radmacher, D. A. Walters, and P. Hillner, Appl. Phys. Lett. 64, 1738-1740 (1994).

[6] S. N. Magonov and D. H. Reneker, Annu. Rev. Mater. Sci. 27, 175-222 (1997).

[7] M. R. Vanlandingham, S. H. McKnight, G. R. Palmese, and J. R. Elings, J. Adhesion 64, 31-59 (1997).

[8] B. J. Briscoe, L. Fiori, and E. Pelillo, J. Phys D. 31, 2395-2405 (1998).

[9] G. Coulon, G. Castelein, and C. G. Sell, Polymer 40, 95-110 (1998).

[10] M. Y. D. Lanzerotti, L. V. Meisel, M. A. Johnson, A. Wolfe, and D. J. Thomson, Mat. Res. Soc. Symp. Proc. 466, 179-184 (1997).

[11] J. Sharma, C. S. Coffey, R. W. Armstrong, W. L. Elban, and M. Y. D. Lanzerotti, in Nanostructure of porosity in laboratory-grown crystals of RDX as revealed by an AFM, Snowbird, Utah, 1999 (AIP Press), p. 719-721.

[12] J. Sharma and C. S. Coffey, in Nature of Ignition sites and hot spots studied by using an atomic force microscope, Seattle, 1996 (AIP Press), p. 811-814.

[13] R. W. Armstrong, C. S. Coffey, V. F. DeVost, and W. L. Elban, J. Appl. Phys. 68 (1990).

[14] F. Baillou, J.M. Dartyge, C. Spyckerelle, and J.Mala, 10th Symposium on Detonation, 816-823 (1993?).

[15] L. Borne, J.-C. Patedoye, and C. Spyckerelle, Propellants, explosives, pyrotechnics 24, 255-259 (1999).

[16] Czerski, H., Proud, W.G. and Field, J.E. "The relationship between shock sensitivity and morphology in granular RDX" Central Eur. J. Energ. Mater. (2006) 3(3) 3-13

[17] Gallier, S. and F. Hiemard, "Microstructure of composite propellants using simulated packings and X-ray tomography." J. Propulsion Power 24 (2008): 154-157.

[18] Zhang, Y., et al. Measuring physical density of explosive charge with γ-ray computed tomography. Theory and Practice of Energetic Materials. 4. L. Chen and C. Feng. Beijing, China Science and Technology Press: (2001) 603-605.

[19] Greenaway, M. W., et al. (2006). X-ray microtomography of sugar and HMX granular beds undergoing compaction. Shock Compression of Condensed Matter - 2005. M. D. Furnish, M. Elert, T. P. Russell and C. T. White. Melville, NY, American Institute of Physics: 1279-1282.

[20] G.M. Swallowe, J.E. Field and L.A. Horn, "Measurements of transient high temperatures during the deformation of polymers.J. Mat. Sci. 21 (1986) 4089-4096

[21] Walley, S. M., D. Xing and J.E. Field. Mechanical properties of three transparent polymers in compression at a very high rate of strain. Impact and Dynamic Fracture of Polymers and Composites. J. G. Williams and A. Pavan. London, Mechanical Engineering Publications Ltd.: 289-303. (1995).

[22] S.M. Walley and J.E. Field, Strain Rate Sensitivity of Polymers in Compression from low to high rates, DYMAT journal 1 No.3,(1994) 211-227

[23] C. R. Siviour, S. M. Walley W.G. Proud and J.E. Field¸ (2005). "The high strain rate compressive behaviour of polycarbonate and polyvinylidene fluoride." Polymer 46: 12546-12555.

[24] D.R. Drodge, D.M. Williamson, S.J.P. Palmer, W.G. Proud and R.K. Govier, The Mechanical Response of a PBX and its binder: combining results across the strain-rate and frequency domains, J. Phys. D.: Appl. Phys. 43 (2010) 335403.

[25] C.R. Siviour and W.G. Proud, Measurements of Strain Propagation in Hopkinson Bar Specimens, Shock Compression of Condensed Matter - 2005. M. D. Furnish, M. Elert, T. P. Russell and C. T. White. Melville, NY, American Institute of Physics, 1293- 1296.

[26] P. J. Rae, S. J. P. Palmer, H.T. Goldrein, A.L. Lewis and J.E. Field, "White-light digital image cross-correlation (DICC) analysis of the deformation of composite materials with random microstructure." Optics Lasers Engng 41: 635-648. (2004)

[27] Siviour, C. R., S. G. Grantham, D.M. Williamson, W.G. Proud, S.M. Walley, J.E. Field (2004). High resolution optical analysis of dynamic experiments on PBXs. Proc. 7th Seminar on New Trends in Research of Energetic Materials. J. Vágenknecht. Pardubice, Czech Republic, University of Pardubice: 277-284.

[28] Siviour, C. R. and W. G. Proud (2007). Damage formation during high strain rate deformation of PBS9501. Shock Compression of Condensed Matter - 2007. M. Elert, M. D. Furnish, R. Chau, N. Holmes and J. Nguyen. Melville, NY, American Institute of Physics: 799-802.

[29] Cornish, R., et al. (2007). Comparison of Porter-Gould constitutive model with compression test data for HTPB/sugar. Shock Compression of Condensed Matter - 2007. M. Elert, M. D. Furnish, R. Chau, N. Holmes and J. Nguyen. Melville, NY, American Institute of Physics: 777-780.

[30] Davison, L. and Graham, R., "Shock Compression of Solids", Physical Reports, Vol. 55, 1979, pp. 255-379.

[31] Rosenberg, Z, Yaziv, D. and Partom, Y.J., "Calibration of Foil-Like Manganin Gauges in Planar Shock Wave Experiments", Journal of Applied Physics, Vol. 51, 1980, pp. 3702-3705.

[32] Rosenberg, Z. and Partom., Y.J., "Lateral Stress Measurement in Shock-Loaded Targets with Transverse Piezoresistance Gauges", Journal of Applied Physics, Vol. 58, 1985, pp. 3072-3076.

[33] Gustavsen, R. L., et al. (2000). Initiation of EDC-37 measured with embedded electromagnetic particle velocity gauges. Shock Compression of Condensed Matter - 1999. M. D. Furnish, L. C. Chhabildas and R. S. Hixson. Melville, New York, American Institute of Physics: 879-882.

[34] Barker, L.M. & Hollenbach, R.E, "Laser Interferometer for Measuring High Velocities of any Reflecting Surface", Journal of Applied Physics, Vol. 43, 1972, pp. 4669-4675.

[35] Briggs, M. E., et al. (2010). Applications and principles of photon-Doppler velocimetry for explosive testing. Proc. 14th Int. Detonation Symposium. S. Peiris, C. Boswell and B. Asay. Arlington, VA, Office of Naval Research: 414-424.

[36] W. J. Carter, and S. P. Marsh (1995). Hugoniot equation of state of polymers. Los Alamos, New Mexico, Los Alamos National Laboratory.

[37] .D Porter, P.J. Gould, J. Phys. IV France, **110** (2003), pp. 809-814.

[38] Porter, D., Gould, P.J., 2006. A general equation of state for polymeric materials. Journal de Physique IV France **134** (2006), 373–378.

[39] E.N. Brown, C.P. Trujillo, G.T. Gray III, P.J. Rae and N.K. Bourne, "Soft Recovery of polytetraflouroethlyene shocked through the crystalline phase II-III transition, J. Appl. Phys 101 (2007) 0249916

[40] D.M. Williamson, D.J. Chapman, W.G. Proud, P.D. Church, "Application of digital speckle radiography to measure the internal displacement fields of a shock loaded material", Photon06 (Institute of Physics) , 4-7th September 2006, Pg. 51.

[41] D M Williamson, C R Siviour, W G Proud, S J P Palmer, R Govier, K Ellis, P Blackwell and C Leppard, Temperature–time response of a polymer bonded explosive in compression (EDC37), J. Phys. D: Appl. Phys. 41 (2008) 085404

[42] 2010 Drodge D.R., Williamson D.M., Palmer S.J.P., Proud W.G. and Govier R.K. (2010) The mechanical response of a PBX and binder: Combining results across the strain-rate and frequency domains, J. Phys. D: Appl. Phys. 43 335403

[43] Porter, D., Gould, P.J., 2006. A general equation of state for polymeric materials. Journal de Physique IV France **134** (2006), 373–378.